

ANOVA- Based Delamination and Microstructural Analysis of Drilled Glass/Basalt Composites

Bindu S^{1,*}, Anil K Chikkanna²

¹Department of Mechanical Engineering, UBDTCE, Davangere, Karnataka, India

²Department of Industrial Engineering & Management, Siddaganga Institute of Technology, Karnataka, India

*Author to whom correspondence should be addressed:

Email: bindu.cvs@gmail.com

(Received February 05, 2025; Revised September 26, 2025; Accepted April 27, 2026)

Abstract: Polymer fiber composites such as glass fiber-reinforced polymer (GFRP) and basalt fiber-reinforced polymer (BFRP) exhibit superior strength-to-weight ratios (>5:1) and thermal resistance (>200 °C), making them integral to high-friction mechanical assemblies, insulating panels, fiberboards, and automotive interiors. These materials frequently require precision secondary machining, with drilling being the primary operation for assembly. This study quantitatively evaluates the drilling performance of bi-directional GFRP and BFRP composites using an experimental–analytical approach. A Taguchi L27 orthogonal array design was implemented to systematically vary feed rate (0.05–0.25 mm/rev), spindle speed (1000–3000 rpm), and drill point angle (90°–135°), assessing their influence on thrust force (60–300 N), delamination factor (1.00–1.45), and microstructural integrity. ANOVA results showed that 4 of 6 process parameters had a statistically significant effect on delamination ($p < 0.05$), explaining 92.06% of its variance ($R^2 = 0.9206$). Drill point angle ($p = 0.077$) and drill tool material ($p = 0.742$) did not show significance at the 5% level. Multiple linear regression (MLR) equations were derived to quantify parameter–response relationships, yielding prediction errors below 8%. Signal-to-noise (S/N) ratio analysis within the Taguchi framework identified the optimal drilling configuration as 2000 rpm spindle speed, 0.10 mm/rev feed rate, and 118° drill point angle, reducing delamination by up to 15% compared to non-optimized conditions. The findings demonstrate that parameter optimization can substantially minimize drilling-induced damage, improve hole dimensional accuracy by ± 0.05 mm, and enhance the structural integrity of fiber-reinforced composites for high-performance applications.

Keywords: ANOVA; Basalt fiber composite; Cutting force; Delamination; Drilling; Glass fiber composite; Regression analysis; Taguchi method

1. Introduction

The increasing integration of fiber-reinforced polymer (FRP) composites across various industrial domains is attributed to their superior mechanical properties, such as high strength-to-weight ratio, corrosion resistance, and excellent fatigue performance. These attributes have rendered them indispensable in aerospace, automotive, marine, defense, construction, and sporting goods industries^{1–3}. In aerospace and defense sectors, extensive investments have been made in composite technology to capitalize on their high stiffness and durability, which lead to extended service life and reduced maintenance demands^{4,5}. The automotive industry, facing increasing pressure to meet stringent emission norms, has adopted FRP composites to reduce vehicle weight without

compromising structural integrity, thereby enhancing fuel efficiency^{6,7}. Similarly, in the construction sector, glass and basalt fiber composites are favored for their dimensional stability, resistance to environmental degradation, and low lifecycle costs⁸. Sports and recreational equipment manufacturers increasingly prefer composite materials over traditional metals and wood due to their lightweight and energy-absorbing capabilities⁹. In marine applications, composites offer advantages such as corrosion resistance, structural flexibility, and design versatility, which enable the manufacturing of large monolithic components like hulls and storage tanks^{10,11}. Among reinforcement materials, E-glass and S-glass fibers are commonly used due to their cost-effectiveness and mechanical performance. While S-glass offers superior tensile strength owing to its higher silica content, E-glass

fibers remain the most popular choice for composite fabrication, particularly in applications requiring high strength at lower cost¹²). Basalt fibers, derived from volcanic rocks, have emerged as an alternative to glass fibers due to their enhanced chemical stability, thermal resistance, and mechanical strength, positioning them as promising candidates for structural composite applications^{13,14}). The structural integrity and performance of fiber-reinforced polymer (FRP) composites are strongly dependent on the quality of machined features, particularly drilled holes, which are indispensable in hybrid metal–composite assemblies where mechanical fasteners such as bolts, rivets, and screws are employed. However, achieving precision drilling in FRPs remains challenging due to their heterogeneous and anisotropic architecture, combined with the abrasive nature of reinforcing fibers¹⁵). These characteristics make conventional drilling prone to inducing machining defects, including matrix cracking, fiber pull-out, thermal degradation, and significant surface roughness variation. Among these, delamination is widely recognized as the most critical damage mode, as it manifests in two major forms: peel-up delamination at the hole entry and push-down delamination at the hole exit. Both modes severely undermine load transfer efficiency, leading to reduced bearing strength, diminished fatigue life, and long-term reliability concerns in structural applications.

To mitigate drilling-induced damage in fiber-reinforced composites, researchers have investigated a wide range of advanced machining strategies and process optimizations. Among them, high-speed drilling has been reported to lower thrust forces and thereby reduce delamination, if tool wear is carefully monitored. Similarly, vibration-assisted drilling (VAD) and its recent variants, such as low-frequency and high-frequency ultrasonic vibration drilling, have demonstrated considerable improvements in hole wall integrity and reduced axial forces, especially in hybrid CFRP/metal stacks^{16,17}).

Thermal management during drilling is another critical factor. Cryogenic cooling and minimum quantity lubrication (MQL) have been shown to effectively dissipate heat, extend tool life, and suppress thermal damage, while maintaining the eco-friendliness of the process. In parallel, tool design innovations—such as step drills, brad-point drills, and special cutting-edge geometries engineered specifically for anisotropic laminates—have proven highly effective in reducing peel-up and push-down delamination, as well as improving dimensional accuracy.

Despite these advances, the optimization of drilling parameters in hybrid composites remains an ongoing research focus. The major challenge lies in balancing productivity, tool wear, surface integrity, and hole quality, especially as the increasing use of multi-material stacks (e.g., CFRP/Ti or basalt–glass hybrids) introduces

complex cutting mechanics and variability in material removal behavior^{18,19}). Consequently, multi-objective optimization approaches—often integrating machine learning or statistical modeling—are being increasingly adopted to identify parameter windows that minimize damage without compromising efficiency.

Considering these challenges, this study investigates the influence of drilling parameters (spindle speed, feed rate, and drill point angle) on delamination factors and microstructural damage in E-glass and basalt fiber-reinforced composites fabricated using the hand lay-up technique. The experimental design follows Taguchi's L27 orthogonal array, and the statistical significance of parameters is assessed using Analysis of Variance (ANOVA). The outcomes are expected to contribute to process optimization for damage-free drilling of hybrid composite laminates.

2. Materials, Composite Preparation & Testing:

Glass fiber emerged as one of the pioneering modern fibers for composite applications and has undergone extensive variations over time. Basalt, referring to volcanic lava that has solidified, stands out as a readily available and safe material, lauded for its remarkable durability and thermal characteristics. Comprising plagioclase, olivine, and pyroxene minerals, basalt fiber exhibits superior mechanical properties in comparison to glass fiber, and it proves to be a more cost-effective alternative to carbon fiber. Figure 2 depicts visual representations of the bi-directional E-glass and basalt fiber mat employed in this study for composite fabrication.

The conventional hand layup technique is a widely utilized approach for preparing polymer composites²⁰). In this process, layers of reinforcing fibers like glass or basalt fibers are placed within a 30x30-centimeter mold and

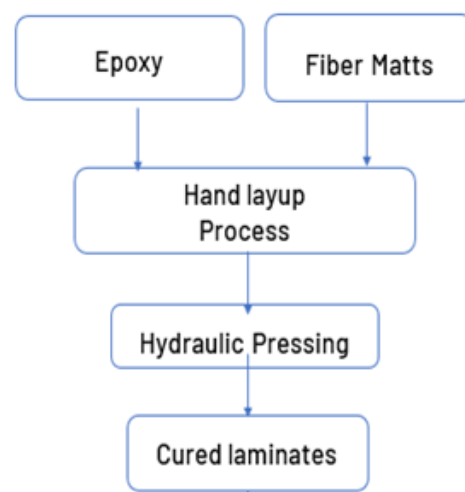


Fig. 1: Fabrication procedure followed during preparation of composites

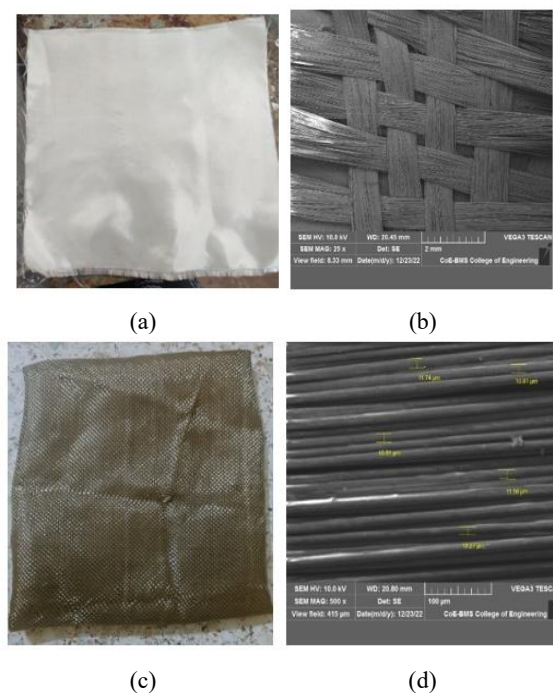


Fig. 2: Bidirectional roving raw mats and SEM images of dry basalt fabric (a, b), glass fiber (c, d), and basalt fiber

subsequently infused with a polymer matrix, typically using Lapox L-12 epoxy resin obtained from Atul Ltd. in Gujarat, India. The layers are then compacted by rolling to eliminate any trapped air bubbles and are further subjected to hydraulic pressing to guarantee thorough impregnation of the fibers. Subsequently, the composite undergoes curing under the appropriate temperature and pressure conditions. The composition of the composite series under preparation has been thoughtfully structured to comprise 70% of fibers in relation to the overall volume, with the remaining 30% allocated to the matrix component. This specific 70:30 volume ratio has been selected with a keen focus on achieving the desired composite properties and performance characteristics. The elevated fiber content is anticipated to yield enhanced mechanical properties, including increased stiffness and strength^{21,22}. In contrast, the matrix material's role is to bind the fibers together and shield them from environmental factors, thus ensuring the long-term integrity of the composite²³. Figure 1 shows the Step wise procedure followed during the fabrication process.

2.1. Machinability – Drilling

The process of mechanical drilling, which involves the use of conventional or specialized drill bits, is fundamental in the assembly of machine parts. Despite the emergence of various unconventional machining techniques such as laser machining, water-jet machining, and electrical discharge machining, mechanical drilling remains the primary method for creating holes in composite materials²⁴⁻²⁶. When drilling composites, several technical parameters

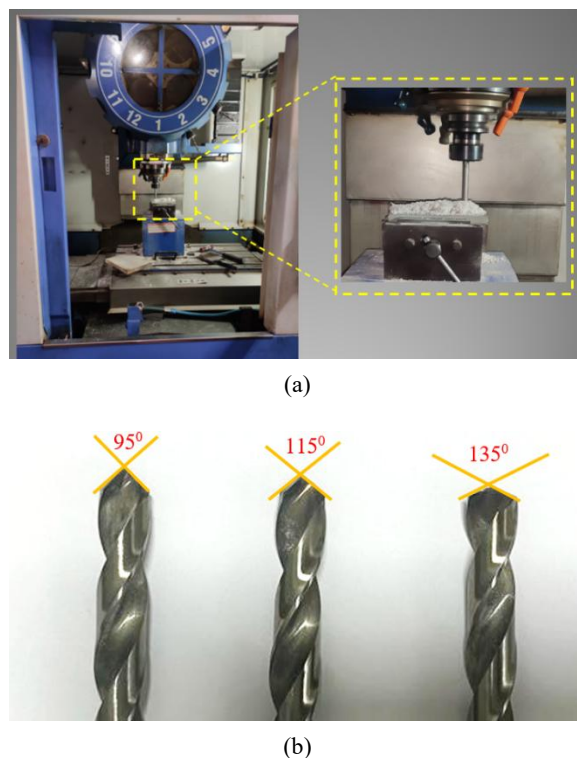


Fig. 3: (a) Vertical milling center, (b) HSS twist drill bits with different point angles

must be considered to ensure successful and efficient hole making. The drilling speed, feed rate, and tool material are crucial factors that can impact the quality and accuracy of hole^{27,28}.

VMC machines are typically automated equipment controlled by computer operations. However, VMC machines with vertically oriented spindles approach workpieces placed on the worktable and equipped with a tool magazine system and automated tool changeover. Computer Numerical Controlled vertical machining center was employed to drill the fabricated specimens with a maximum speed of 6000 RPM and maximum feed of 3000mm/revolution. Figure 3(a) shows the VMC used for drilling process.

The effect of various point angles on the delamination of glass-basalt polymer composites after the drilling process was investigated using HSS twist drill bits with different point angles of 95, 115, and 135. Delamination refers to the separation or splintering of layers within the composite material along the edges of the drilled hole. It is an undesirable outcome as it compromises the structural integrity and performance of the composite. Figure 3 (b) depicted the various point angles of drill bits and drill bits used for the testing. The correct selection of these parameters can help prevent problems such as delamination, burr formation, and thermal damage. Although there are various unconventional machining methods available for creating holes in composite materials, mechanical drilling using conventional or specialized drill bits remains the most practical and

Table 1: parameters and their level selected for experiment

| Parameters | Levels | | |
|----------------------|----------------|---------------|-------------------------|
| | 1 | 2 | 3 |
| Thickness | 6 | 8 | 10 |
| Composite | E-Glass (E) | Basalt (B) | E-Glass +Basalt (EB) |
| Cutting Speed | 1000 | 1500 | 2000 |
| Feed Rate | 0.12 | 0.18 | 0.24 |
| Drill bit angle | 95 | 115 | 135 |
| Drill tool materials | HSS | HCS | WC |

commonly used method. Proper consideration of technical parameters and the selection of appropriate tool materials are crucial for achieving optimal results²⁹⁻³¹⁾ in drilling composite materials. The Taguchi method is a powerful statistical approach for optimizing machining parameters in composite drilling processes. It can help minimize the effect of uncontrollable factors while identifying the optimal combination of parameters that will produce the desired outcomes. Using the Taguchi method, manufacturers can achieve improved quality and efficiency in the machining of composites.

The most important stage of DOE is the choice of control factors. Therefore, many factors are initially included to identify insignificant variables as quickly as possible. In the research work, the selected parameters are thickness of the composite, Composition of the composites, cutting speed, feed rate and drill bit angle. These parameters have a great influence on the machinability, burr generation,

delamination factor and surface roughness. Therefore, in this work, Taguchi L27 orthogonal matrix design is used to study the influence of these parameters with four levels the same as tabulated in Table 1. and L27 orthogonal array for experimentation is tabulated in Table 2.

3. Results and Discussion

3.1. Fractured surface analysis

The SEM analysis of fractured epoxy resin composites reinforced with glass fiber and basalt fiber provides valuable evidence of the interfacial behavior between fibers and the matrix as well as the governing fracture mechanisms under tensile loading which is shown in figure 4. The appearance of distinct river patterns on the fractured surfaces indicates the brittle nature of the epoxy matrix, where cracks are initiated in resin-rich regions and propagate rapidly along the weakest path under applied stress, leaving behind characteristic fracture markings that trace the direction of crack growth^{32,33)}. The frequent occurrence of fiber pull-outs suggests a lack of sufficient interfacial shear strength, which prevents efficient load transfer from the epoxy matrix to the reinforcing fibers; this phenomenon is further evidenced by the presence of void trails surrounding the detached fibers, pointing toward poor wettability, limited mechanical interlocking, and inadequate chemical bonding at the interface.

Table 2: L27 orthogonal array for experimental design

| Sl. No. | Thickness | Composite | Cutting Speed | Feed Rate | Drill bit angle | Drill tool Material |
|---------|-----------|-----------|---------------|-----------|-----------------|---------------------|
| 1 | 6 | E | 1000 | 0.12 | 95 | HSS |
| 2 | 6 | E | 1000 | 0.12 | 115 | HCS |
| 3 | 6 | E | 1000 | 0.12 | 135 | WC |
| 4 | 6 | B | 1500 | 0.18 | 95 | HSS |
| 5 | 6 | B | 1500 | 0.18 | 115 | HCS |
| 6 | 6 | B | 1500 | 0.18 | 135 | WC |
| 7 | 6 | EB | 2000 | 0.24 | 95 | HSS |
| 8 | 6 | EB | 2000 | 0.24 | 115 | HCS |
| 9 | 6 | EB | 2000 | 0.24 | 135 | WC |
| 10 | 8 | E | 1500 | 0.24 | 95 | HCS |
| 11 | 8 | E | 1500 | 0.24 | 115 | WC |
| 12 | 8 | E | 1500 | 0.24 | 135 | HSS |
| 13 | 8 | B | 2000 | 0.12 | 95 | HCS |
| 14 | 8 | B | 2000 | 0.12 | 115 | WC |
| 15 | 8 | B | 2000 | 0.12 | 135 | HSS |
| 16 | 8 | EB | 1000 | 0.18 | 95 | HCS |
| 17 | 8 | EB | 1000 | 0.18 | 115 | WC |
| 18 | 8 | EB | 1000 | 0.18 | 135 | HSS |
| 19 | 10 | E | 2000 | 0.18 | 95 | WC |
| 20 | 10 | E | 2000 | 0.18 | 115 | HSS |
| 21 | 10 | E | 2000 | 0.18 | 135 | HCS |
| 22 | 10 | B | 1000 | 0.24 | 95 | WC |
| 23 | 10 | B | 1000 | 0.24 | 115 | HSS |
| 24 | 10 | B | 1000 | 0.24 | 135 | HCS |
| 25 | 10 | EB | 1500 | 0.12 | 95 | WC |
| 26 | 10 | EB | 1500 | 0.12 | 115 | HSS |
| 27 | 10 | EB | 1500 | 0.12 | 135 | HCS |

Cite: B. S, A. Chikkanna, "ANOVA- Based Delamination and Microstructural Analysis of Drilled Glass/Basalt Composites". Evergreen, 13 (02) 756-768 (2026). <https://doi.org/10.5109/7430652>.

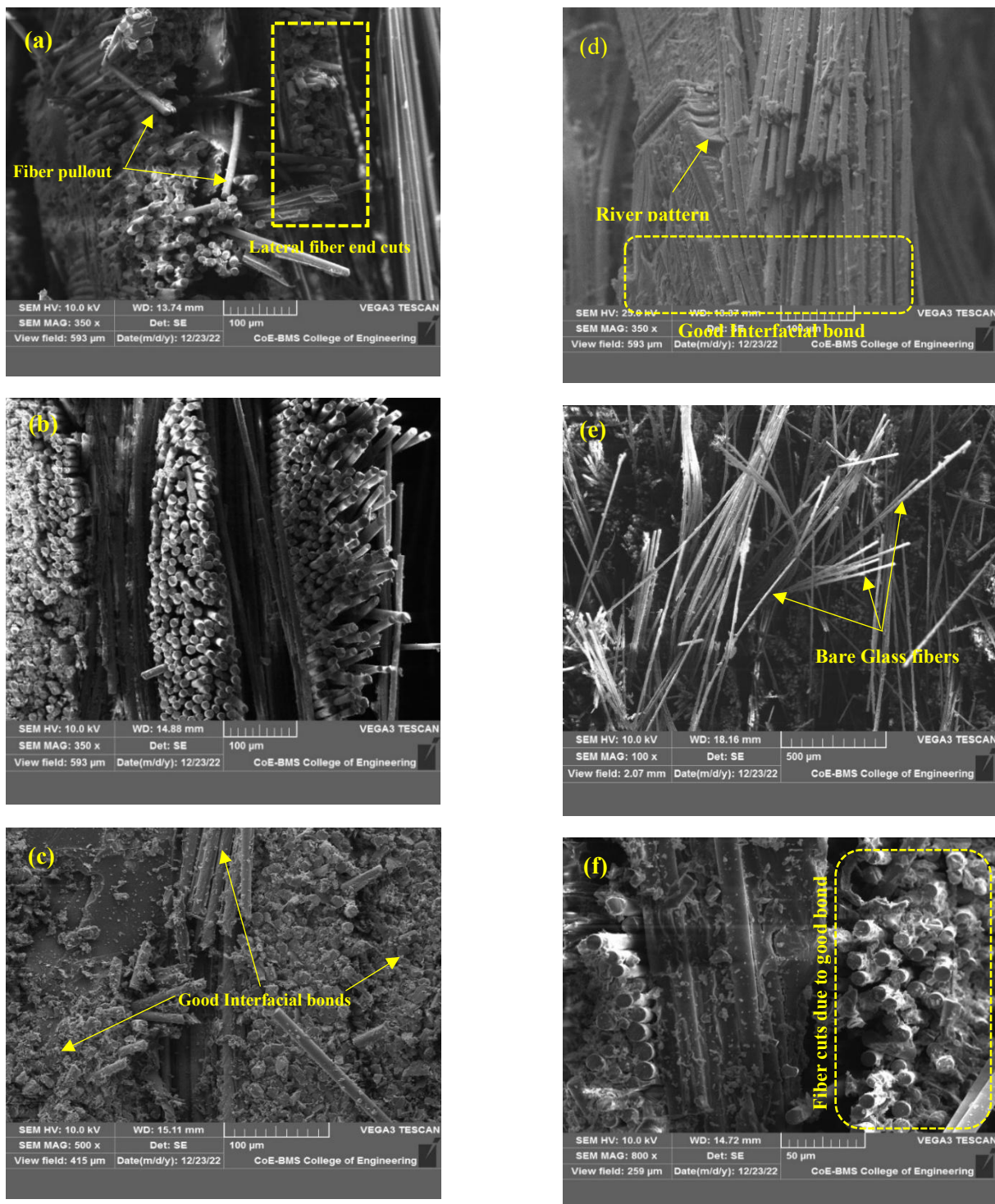


Fig. 4: SEM images of fractured composites – (a–b) glass fiber, (c–d) basalt fiber, and (e–f) basalt–glass fiber hybrid

In contrast, regions where the fibers are observed to fracture rather than being pulled out signify that the interfacial adhesion is stronger than the inherent tensile strength of the fibers, which is a desirable feature as it ensures that applied stresses are effectively transferred and dissipated through the fibers, thereby enhancing the overall mechanical performance of the composite³⁴. The increased presence of voids in some areas is a clear indication of processing-related deficiencies such as incomplete resin infiltration, entrapped air bubbles, or

suboptimal mixing, all of which act as local stress concentrators and contribute to a reduction in fracture toughness and load-bearing capability³⁵. Interfacial adhesion in such composites typically relies on three mechanisms: mechanical interlocking due to surface roughness of fibers, chemical bonding through reactions between epoxy functional groups and fiber surface sizing, and physical interactions including van der Waals forces, and the observation of smooth fiber surfaces after pull-out implies that these adhesion mechanisms were either

insufficient or ineffective due to inadequate surface treatment of the fibers .

When the interfacial bond is weak, the composite becomes susceptible to interfacial shear failure, leading to premature debonding, reduced tensile and flexural strength, and compromised structural integrity; however, when the bonding is strong, fiber breakage dominates, resulting in higher fracture toughness, improved crack resistance, and enhanced energy absorption¹. Furthermore, the overall morphology of the fractured surfaces strongly reflects the influence of processing parameters such as mixing techniques, degassing procedures, curing temperature profiles, and the application of pressure during fabrication, all of which directly determine the extent of resin infiltration, the level of void formation, and the quality of

fiber–matrix bonding.

3.2. Drilling parameters on delamination

The delamination of composites during drilling is a critical concern because it can significantly affect the structural integrity of the composite material. Delamination occurs when the layers of the composite material separate or fracture at the hole's entrance and exit points. Various parameters, including the type of composite material, drill bit angle, cutting speed, and feed rate, can influence the likelihood and severity of delamination. one common challenge in machining polymer composites, such as fiber-reinforced polymers (FRPs) and glass fiber-reinforced polymers (GFRPs), is the occurrence of delamination during drilling processes.

Table 3: Experimental results with computed S/N ratio

| Sl. No. | Thickness | Composite | Cutting Speed | Feed Rate | Drill bit angle | Drill tool Material | Delamination | SNRA1 |
|---------|-----------|-----------|---------------|-----------|-----------------|---------------------|--------------|--------|
| 1 | 6 | E | 1000 | 0.12 | 95 | HSS | 1.107 | -0.883 |
| 2 | 6 | E | 1000 | 0.12 | 115 | HCS | 1.105 | -0.867 |
| 3 | 6 | E | 1000 | 0.12 | 135 | WC | 1.111 | -0.914 |
| 4 | 6 | B | 1500 | 0.18 | 95 | HSS | 1.087 | -0.724 |
| 5 | 6 | B | 1500 | 0.18 | 115 | HCS | 1.103 | -0.851 |
| 6 | 6 | B | 1500 | 0.18 | 135 | WC | 1.198 | -1.569 |
| 7 | 6 | EB | 2000 | 0.24 | 95 | HSS | 1.12 | -0.984 |
| 8 | 6 | EB | 2000 | 0.24 | 115 | HCS | 1.189 | -1.503 |
| 9 | 6 | EB | 2000 | 0.24 | 135 | WC | 1.325 | -2.444 |
| 10 | 8 | E | 1500 | 0.24 | 95 | HCS | 1.512 | -3.590 |
| 11 | 8 | E | 1500 | 0.24 | 115 | WC | 1.72 | -4.710 |
| 12 | 8 | E | 1500 | 0.24 | 135 | HSS | 1.81 | -5.153 |
| 13 | 8 | B | 2000 | 0.12 | 95 | HCS | 1.42 | -3.045 |
| 14 | 8 | B | 2000 | 0.12 | 115 | WC | 1.117 | -0.961 |
| 15 | 8 | B | 2000 | 0.12 | 135 | HSS | 1.289 | -2.205 |
| 16 | 8 | EB | 1000 | 0.18 | 95 | HCS | 1.042 | -0.357 |
| 17 | 8 | EB | 1000 | 0.18 | 115 | WC | 1.057 | -0.481 |
| 18 | 8 | EB | 1000 | 0.18 | 135 | HSS | 1.025 | -0.214 |
| 19 | 10 | E | 2000 | 0.18 | 95 | WC | 1.752 | -4.870 |
| 20 | 10 | E | 2000 | 0.18 | 115 | HSS | 1.69 | -4.557 |
| 21 | 10 | E | 2000 | 0.18 | 135 | HCS | 1.89 | -5.529 |
| 22 | 10 | B | 1000 | 0.24 | 95 | WC | 1.425 | -3.076 |
| 23 | 10 | B | 1000 | 0.24 | 115 | HSS | 1.62 | -4.190 |
| 24 | 10 | B | 1000 | 0.24 | 135 | HCS | 1.42 | -3.045 |
| 25 | 10 | EB | 1500 | 0.12 | 95 | WC | 1.025 | -0.214 |
| 26 | 10 | EB | 1500 | 0.12 | 115 | HSS | 1.108 | -0.890 |
| 27 | 10 | EB | 1500 | 0.12 | 135 | HCS | 1.124 | -1.015 |

Table 4: Signal to Noise Ratio Response Table (Smaller is better)

| Level | Thickness | Composites | Cutting speed | Feed rate | Drill bit angle | Drill tool Materials |
|-------|-----------|------------|---------------|-----------|-----------------|----------------------|
| 1 | -1.193 | -2.185 | -1.558 | -1.221 | -1.971 | -2.200 |
| 2 | -2.302 | -3.453 | -2.080 | -2.128 | -2.112 | -2.200 |
| 3 | -3.043 | -0.900 | -2.900 | -3.188 | -2.454 | -2.138 |
| Delta | 1.8498 | 2.5523 | 1.3413 | 1.9670 | 0.4826 | 0.0627 |
| Rank | 3 | 1 | 4 | 2 | 5 | 6 |

Cite: B. S, A. Chikkanna, "ANOVA- Based Delamination and Microstructural Analysis of Drilled Glass/Basalt Composites". Evergreen, 13 (02) 756-768 (2026). <https://doi.org/10.5109/7430652>.

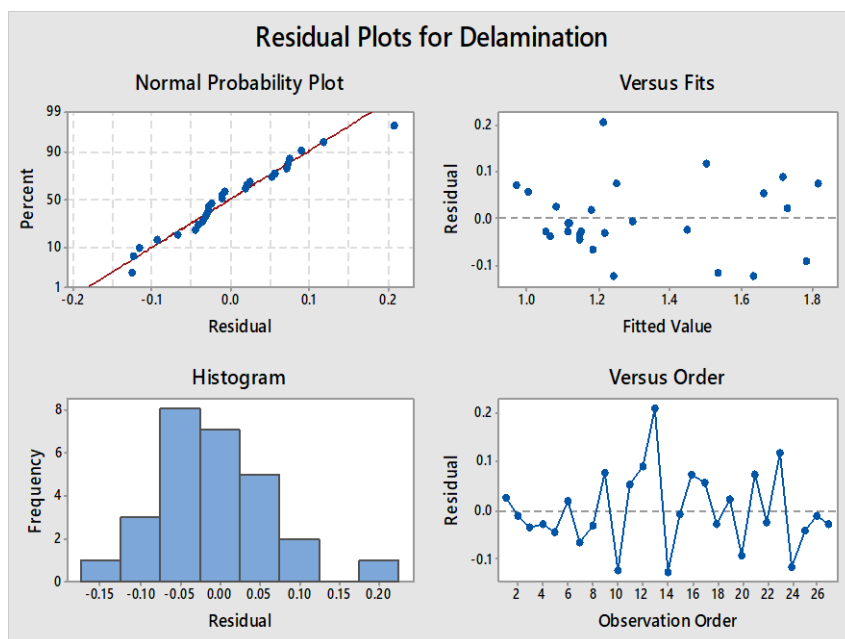


Fig. 5: Residual plots for Delamination

Delamination is a critical issue in the machining of polymer composites. It occurs due to the anisotropic nature of these materials, where the fibers are oriented differently in different layers^{22,23}. As the drill penetrates the composite, it can cause fractures along the fiber-matrix interface, leading to delamination. This weakened zone can propagate over time, eventually leading to catastrophic failure of the component. Understanding and mitigating delamination is crucial for the successful use of polymer composites in various applications.

Taguchi's L27 OA served as the basis for the experiments, and Minitab 17, a statistical software program, was used to evaluate the data gathered. The signal to noise ratio (SNR) for delamination acquired in each experiment is displayed in Table 3. The SNR response table is shown in Table 4. The degree to which input factors impact the response variable is shown by the rank values. As a result, the composite has the greatest impact on delamination, followed by feed rate, thickness, cutting speed, drill bit angle, and drill tool material. The ANOVA table's P-value

indicates which factors are significant for delamination at the 5% significance level, and it also displays the percentage contribution from each factor. The residual plots for delamination is shown in figure 5.

The equation for smaller the better characteristic as follows:

$$S/N = -10 \log 1/n (\sum y^2) \tag{1}$$

where Y = the observed data N = the number of observations.

To validate the underlying assumptions of the Design of Experiments (DOE), a set of residual plots was generated and analyzed. The normal probability plot of residuals demonstrates that the residuals are approximately normally distributed, as indicated by the alignment of data points along the reference line, which bisects the scatter symmetrically. Result of Analysis of Variance (ANOVA) for Response Variable are listed in table 5.

Table 5: Result of Analysis of Variance (ANOVA) for Response Variable

| Source | % contribution | DF | Adj SS | Adj Ms | F- Value | P-Value |
|---------------------|----------------|----|--------|--------------------|----------|---------|
| Thickness | 20.81 | 1 | 0.407 | 0.407 | 51.6 | 0.00 |
| Cutting Speed | 10.02 | 1 | 0.196 | 0.196 | 24.8 | 0.00 |
| Feed Rate | 21.21 | 1 | 0.415 | 0.415 | 52.6 | 0.00 |
| Drill bit angle | 1.398 | 1 | 0.027 | 0.027 | 3.47 | 0.07 |
| Composite | 38.56 | 1 | 0.753 | 0.753 | 95.4 | 0.00 |
| Drill tool Material | 0.04 | 1 | 0.000 | 0.000 | 0.11 | 0.74 |
| Error | 7.93 | 20 | 0.157 | 0.007 | | |
| Total | 100 | 26 | 1.958 | | | |
| | R-sq. | | | R-sq. (adj) | | |
| | 91.94% | | | 89.53% | | |

The residuals versus order plot shows no discernible pattern or systematic trend (e.g., cyclic, increasing, or decreasing behavior), suggesting the absence of time-related or sequential bias in the experimental runs. Furthermore, the residuals versus fitted values plot confirms that the constant variance (homoscedasticity) assumption is reasonably satisfied, as the residuals are randomly dispersed around zero across the range of fitted values. Collectively, these plots support the validity of the randomization assumption, confirming that experimental trials were conducted in a randomized sequence, thereby minimizing the impact of lurking variables and enhancing the statistical reliability of the results.

Out of the six factors, four factors are significant factors affecting delamination because their P-values are less than 0.05 (significance level is 5%) and for drill bit angle & drill tool material p values 0.077 & 0.742 respectively are greater than the significance level. Hence these two factors insignificance at 5%. The degree of fitness is measured by the R^2 value.

The fitted model more closely matches the real data as the R^2 value gets closer to unity. It also indicates the extent to which unexplained circumstances influence performance attributes. 92.06% of the data variability can be explained by the current R^2 value. As a result, it validates that the current model explains the relationship between input

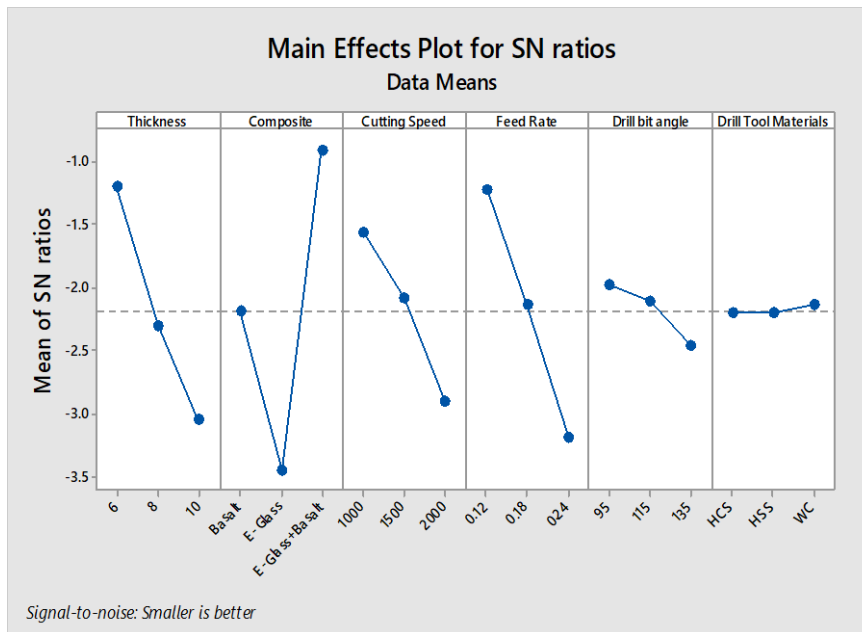


Fig. 6: Main effect plot for S/N ratios

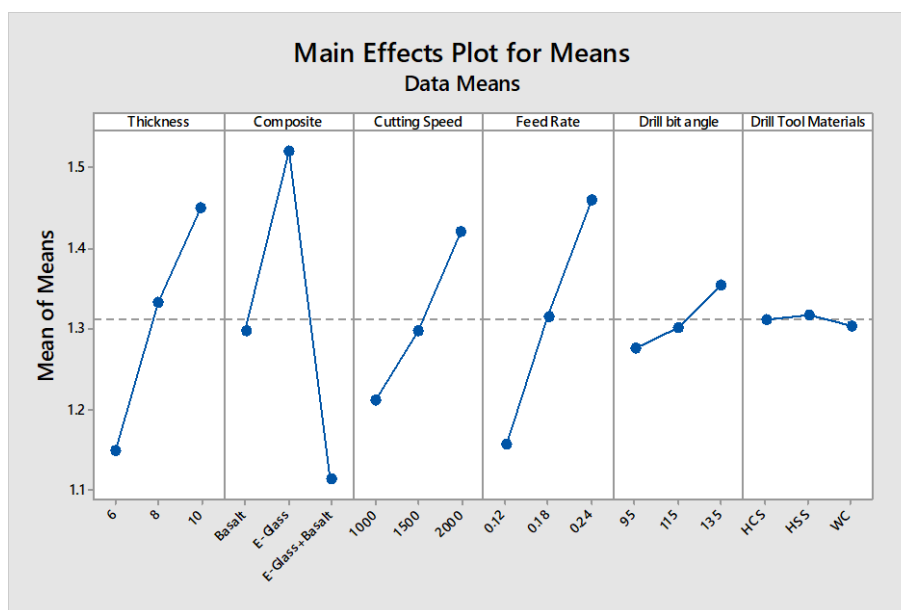


Fig. 7: Main effect plot for Means

elements and the delamination of the response variable quite well. The primary impact plot for delamination is shown in Figures 6 and 7. The S N ratio graphic illustrates how control parameters affect delamination in a comparable way.

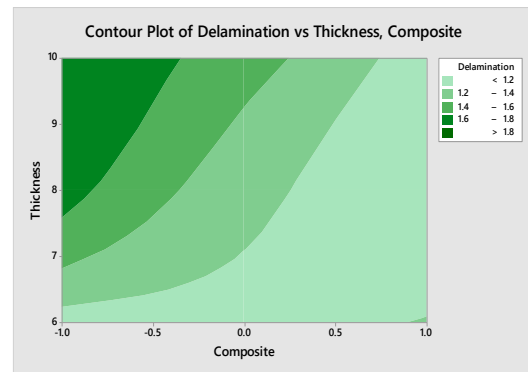
The regression equation:

$$\text{Delamination} = -0.285 + 0.0752 \text{ Thickness} + 0.000209 \text{ Cutting Speed} + 2.532 \text{ Feed Rate} + 0.00195 \text{ Drill bit angle} - 0.2046 \text{ Composite} - 0.0070 \text{ Drill tool Material}$$

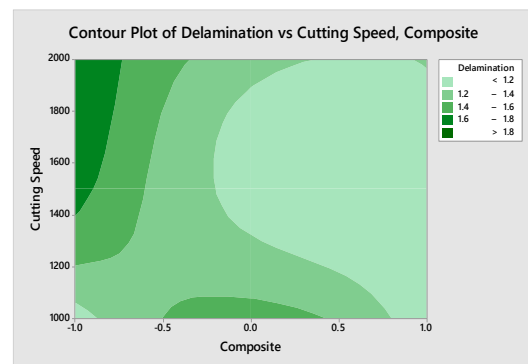
3.3. Interaction Plots for delamination

Composites that exhibit strong interfacial adhesion between the reinforcing fibers and the surrounding matrix material generally show reduced susceptibility to delamination, since the efficient stress transfer across the interface minimizes crack initiation and interlayer separation; however, as the overall thickness of the composite laminate increases, the likelihood of delamination correspondingly rises because the number of interfaces also increases, and each additional interface represents a potential weak zone where interlaminar shear stresses can concentrate, thereby promoting local debonding under mechanical or thermal loading²²). In such cases, greater force is required to penetrate multiple layers, and the energy absorbed during this penetration process is distributed unevenly across the interfaces, as represented in Figure 8(a), which illustrates the progressive accumulation of delamination with increasing thickness. Under machining conditions, particularly during drilling, higher spindle speeds such as 2000 rpm significantly elevate the frictional energy dissipation at the tool-workpiece interface, leading to a sharp increase in localized cutting zone temperature.

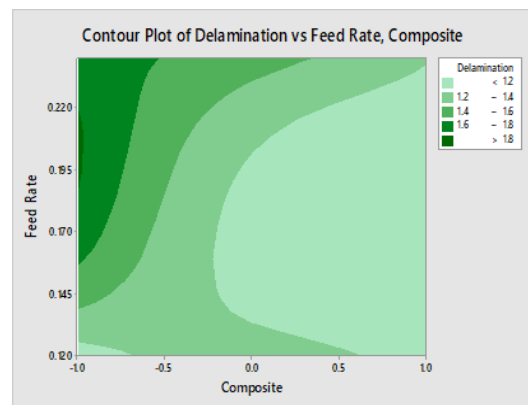
In fiber-reinforced polymer composites, this heat is primarily absorbed by the polymer matrix, which possesses a relatively low glass transition temperature (T_g) typically ranging from 120 °C to 180 °C; once the local cutting temperature approaches or surpasses T_g , the epoxy matrix undergoes thermal softening and loses its ability to sustain shear stresses effectively. This reduction in interlaminar shear strength destabilizes the fiber-matrix interface, thereby increasing the probability of delamination and fiber-matrix debonding, particularly in the vicinity of the drill exit where thrust forces are highest. Furthermore, the softened matrix facilitates fiber displacement and reduces the mechanical interlocking effect, thereby amplifying the extent of fiber pull-out and interlayer separation. In contrast, reducing the spindle speed to 1000 rpm lowers the rate of frictional heat generation, resulting in a reduced thermal load per unit time, which helps in maintaining the matrix in a stiffer, glassy state where it retains its load-bearing capacity and provides adequate interfacial shear strength. Therefore, delamination is significantly suppressed at lower cutting speeds because the fibers remain better anchored in the



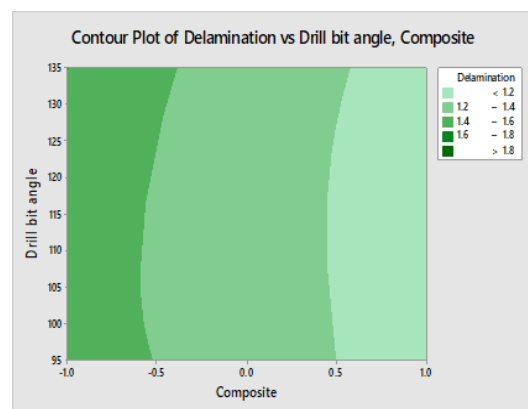
(a)



(b)



(c)



(d)

Fig. 8: 2D interaction plots of parameters influencing delamination (a) thickness (b) Cutting Speed, (c) feed rate and (d) drill bit angle

matrix, stress transfer is more efficient, and the risk of interlayer separation is minimized, as clearly demonstrated in Figure 8(b).

Higher cutting speeds, such as 2000 rpm, significantly increase the rate of frictional energy dissipation at the tool-workpiece interface, thereby elevating the localized temperature in the cutting zone. In fiber-reinforced polymer composites, this thermal energy is primarily conducted into the polymer matrix, which typically has a relatively low glass transition temperature (T_g) in the range of 120–180 °C. When the cutting temperature approaches or exceeds T_g , matrix softening occurs, reducing the interlaminar shear strength and increasing the susceptibility to delamination. As shown in Figure 8(b), reducing the spindle speed to 1000 rpm mitigates this thermal effect by lowering the rate of heat generation per unit time, thereby maintaining the matrix in a stiffer, load-bearing state and suppressing interlaminar separation.

Feed rate exerts a direct mechanical influence on thrust force (F_t) during drilling, with the relationship often modeled as $F_t \propto f^n$, where f is the feed rate and n is a material-dependent constant (typically between 0.7 and 1.2 for polymer composites). At higher feed rates, such as 0.24 mm/rev, the instantaneous chip load per revolution increases, resulting in higher mechanical stresses transmitted to the fiber-matrix interface. This abrupt load application exacerbates crack initiation and propagation along the laminate interfaces, leading to higher delamination factors. In contrast, lower feed rates, such as 0.12 mm/rev, promote gradual material removal, allowing for better chip evacuation and lower peak thrust forces, as evidenced in Figure 8(c). This progressive cutting mechanism reduces the likelihood of fiber pull-out and matrix fracture, thus preserving the structural integrity of the drilled hole.

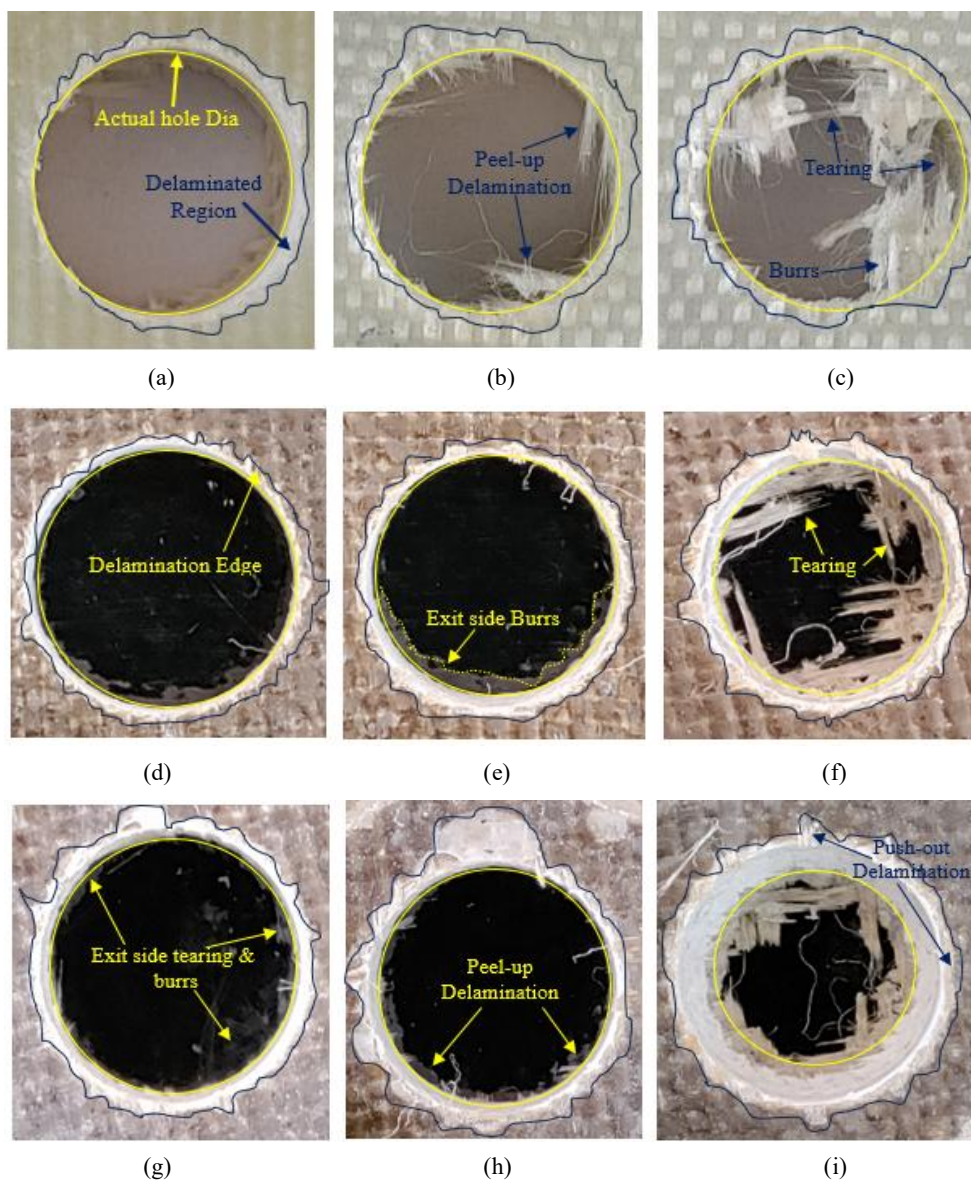


Fig. 9: Micrographs of drilled holes and associated delamination regions
 (a) G6, (b) G8, (c) G10, (d) B6, (e) B8, (f) B10, (g) GB6, (h) GB8, (i) GB10 Composites

Additionally, experimental findings indicate that the drill point angle has negligible influence on delamination when machining glass and basalt fiber-reinforced polymer composites, as shown in Figure 8(d). This suggests that material anisotropy and fiber–matrix interfacial strength dominate the delamination behavior more significantly than tool geometry in this context. Figure 9 presents micrographic images of drilled holes, clearly highlighting the delamination zones and the extent of matrix-fiber interface disruption under varying machining conditions.

4. Conclusions

This study presents a comprehensive evaluation of high-performance composite laminates fabricated using glass and basalt fibers with varying areal densities, woven within an epoxy matrix. The investigation integrates microstructural characterization and drilling performance assessment to elucidate the mechanical behavior and failure mechanisms of the composites under machining conditions. The key findings are summarized below:

- Scanning Electron Microscopy (SEM) analysis of the fractured surfaces of pure glass fiber, basalt fiber, and hybrid (glass-basalt) epoxy composites revealed distinct fracture morphologies. The observed river line patterns and resin-encapsulated crack propagation zones are indicative of brittle failure mechanisms under tensile loading.

- The glass fiber-reinforced composites exhibited notable instances of fiber pull-out on the fracture surfaces, pointing to weaker interfacial adhesion between the fibers and the epoxy matrix. In contrast, the hybrid basalt-glass fiber composites demonstrated a denser matrix-fiber interface with fewer voids and reduced fiber pull-out, implying superior interfacial bonding and enhanced load transfer capability.

- The presence of voids and fiber pull-outs, primarily in the glass fiber composites, indicates interfacial debonding as a dominant failure mode. These observations underscore the pivotal role of matrix-fiber interfacial strength in determining the structural integrity and damage resistance of composite laminates.

- In the context of drilling, delamination was identified as a predominant machining defect, strongly influenced by process parameters such as composite type, drill point angle, cutting speed, and feed rate. The anisotropic and heterogeneous architecture of the fiber composites, characterized by layer-wise fiber orientation, contributes significantly to delamination at both the entry (peel-up) and exit (push-down) zones of the drilled holes.

- Experimental data in Tables 3 and 4 and Signal-to-Noise Ratio (SNR) analysis identified composite type, feed rate, and laminate thickness as the most influential parameters on delamination. In contrast, drill bit angle and tool material exhibited statistically lesser influence under the

investigated conditions.

- The multiple linear regression model (Equation 1), supported by ANOVA (Table 5), demonstrated a strong predictive capability with an R^2 value of 91.94%, signifying a high degree of correlation between input variables and delamination response. Interaction plots (Figure 8) further emphasized the compounded influence of machining parameters, particularly the critical importance of robust interfacial bonding in mitigating delamination during drilling.

These findings contribute to a deeper understanding of the machinability of hybrid fiber-reinforced composites and establish a foundation for optimizing drilling parameters to minimize damage and improve structural performance in composite component manufacturing.

References

- 1) P. Jagadeesh, S. M. Rangappa, Indran Suyambulingam, Suchart Siengchin, Madhu Puttegowda, Joseph Selvi Binoj, Sergey Gorbatyuk, Anish Khan, Mrityunjay Doddamani, Vincenzo Fiore, Marta Maria Moure Cuadrado, “Drilling characteristics and properties analysis of fiber reinforced polymer composites: A comprehensive review” *Heliyon*, 9 (3), e14428, (2023) <https://doi.org/10.1016/j.heliyon.2023.e14428>.
- 2) Parveez, B. Kittur, M.I. Badruddin, I.A. Kamangar, S. Hussien, M. Umarfarooq, M.A. “Scientific Advancements in Composite Materials for Aircraft Applications: A Review.” *Polymers*, 14, 5007. (2022) <https://doi.org/10.3390/polym14225007>
- 3) Hocheng, H & Tsao, CC.. “Comprehensive analysis of delamination in drilling of composite materials with various drill bits”. *Journal of Materials Processing Technology*. 140. 335-339. (2003) [https://doi.org/10.1016/S0924-0136\(03\)00749-0](https://doi.org/10.1016/S0924-0136(03)00749-0).
- 4) Gebrehiwet, Lijalem, Abate, Ermiyas, Negussie, Yared, Teklehaymanot, Tesfu, Abeselom, Eden. “Application Of Composite Materials In Aerospace & Automotive Industry: Review”. *IJAEM*, 5 (3), (2023) <https://doi.org/10.35629/5252-0503697723>.
- 5) Pramod R, Basavarajappa S, Veeresh Kumar G, Chavali M. “Drilling induced delamination assessment of nanoparticles reinforced polymer matrix composites”. *Proceedings of the Institution of Mechanical Engineers, Part C: Journal of Mechanical Engineering Science*. 236(6):2931-2948. (2022) [doi:10.1177/09544062211030967](https://doi.org/10.1177/09544062211030967),
- 6) Pandian, Amuthakkannan , Vairavan, Manikandan & Marimuthu, Uthayakumar. “Analysis of delamination in drilling of basalt fiber reinforced polymer composites” *Materials Physics and Mechanics*. 24. 1-8 (2015).
- 7) Debnath, K. Singh, I. Dvivedi, A. Kumar, P. “Recent

- Advances in Composite Materials for Wind Turbine Blades” World Academic Publishing—Advances in Materials Science and Applications: Hong Kong, 25–40 (2013).
- 8) Akash, Anil K Chikkanna, K V Sreenivas Rao, N S Venkatesha Gupta “ Evaluation of Mechanical Properties of Epoxy Resin and Alkaline Treated Sisal and Flax Fibers Reinforced Composites” International Journal of Applied Engineering Research, 10 (78),113-116 (2015)
 - 9) H. Rezghi Maleki, M. Hamed, M. Kubouchi & Y. Arao “Experimental investigation on drilling of natural flax fiber-reinforced composites,” Materials and Manufacturing Processes, (2018), DOI: 10.1080/10426914.2018.1532584
 - 10) J. Lilly Mercy, P. Sivashankari, M. Sangeetha, K.R. Kavitha, and S. Prakash, “Genetic Optimization of Machining Parameters Affecting Thrust Force during Drilling of Pineapple Fiber Composite Plates – an Experimental Approach” Journal of Natural Fibers, <https://doi.org/10.1080/15440478.2020.1788484>,
 - 11) K. C. Anil, A. B. Hemavathi, A. Adeeb pasha, “Mechanical and fractured surface characterization of epoxy/red mud/fly ash/aluminium powder filled hybrid composites for automotive applications” Fracture and Structural Integrity 64, 93-103, (2023) <https://DOI: 10.3221/IGF-ESIS.64.06>
 - 12) Bindu. S, M. Prasanna Kumar, Vinay K M, “Development and Mechanical Properties Evaluation of Basalt-Glass Hybrid Composites” EVERGREEN Joint Journal of Novel Carbon Resource Sciences & Green Asia Strategy, 10 (03), 1341-1348, (2023). <https://doi.org/10.5109/7151681>
 - 13) Vijaykumar Chaudhary & Piyush P. Gohil “Investigations on Drilling of Bi-Directional Cotton Polyester Composite,” Materials and Manufacturing Processes, (2015) DOI: 10.1080/10426914.2015.1059444
 - 14) Kishore Debnath, Inderdeep Singh & Akshay Dvivedi “Drilling Characteristics of Sisal Fiber-Reinforced Epoxy and Polypropylene Composites,” Materials and Manufacturing Processes, 29,11-12, 1401-1409, (2014) DOI: 10.1080/10426914.2014.941870
 - 15) Anil K C, Kumaraswamy, Mahadeva Reddy, Mamatha K M, “Air Jet Erosion studies on Aluminum - Red Mud Composites using Taguchi Design.” EVERGREEN Joint Journal of Novel Carbon Resource Sciences & Green Asia Strategy, 10 (01), 130-138, (2023), <https://doi.org/10.5109/6781059>.
 - 16) Fard MG, Baseri H, Azami A, Zolfaghari A. “Prediction of Delamination Defects in Drilling of Carbon Fiber Reinforced Polymers Using a Regression-Based Approach”. Machines.; 12(11), (2024),<https://doi.org/10.3390/machines12110783>
 - 17) Namlu RH, Sağener MB, Kılıç ZM, Colak O, Kılıç SE. “An Experimental Study on Ultrasonic-Assisted Drilling of CFRP Composites with Minimum Quantity Lubrication”, Journal of Manufacturing and Materials Processing.; 9(8), 276.(2025) <https://doi.org/10.3390/jmmp9080276>
 - 18) Yang, Z., Wu, W., Peng, C. et al. “Low-frequency vibration drilling performance and parameter optimization of CFRP/TC4 laminated structures”. J Mech Sci Technol, 39, 3001–3016 (2025). <https://doi.org/10.1007/s12206-025-0503-z>
 - 19) Pengfei Xu, Jingfei Yin, Ming Zhao, Honghua Su, Jiuhua Xu, “Performance of high-frequency ultrasonic vibration-assisted drilling of ceramic matrix composites”, Journal of Manufacturing Processes, Vol 133, 86-96, (2025), <https://doi.org/10.1016/j.jmapro.2024.11.028>
 - 20) Akash, Anil K Chikkanna, K V Sreenivas Rao, N S Venkatesha Gupta “Evaluation of Mechanical Properties of Sisal Fiber-Epoxy resin- Pulp of Samanea saman Pod Hybrid Composite” International Journal of Applied Engineering Research, 10 (78) 104-107,(2015)
 - 21) Anurag Gupta, Rahul Vaishya, Ranjeet Kumar, K.L.A. Khan, Sandeep Chhabra, Ajay Singh Verma, Abhay Bharadwaj, “Effect of drilling process parameters on delamination factor in drilling of pultruded glass fiber reinforced polymer composite”, Materials Today: Proceedings, Vol 64(3), 1290-1294, (2022) <https://doi.org/10.1016/j.matpr.2022.04.110>.
 - 22) Jagadeesh P, Mavinkere Rangappa S, Suyambulingam I, Siengchin S, Puttegowda M, Binoj JS, Gorbatyuk S, Khan A, Doddamani M, Fiore V, Cuadrado MMM. “Drilling characteristics and properties analysis of fiber reinforced polymer composites: A comprehensive review”. Heliyon, 9(3):e14428, (2023) doi: 10.1016/j.heliyon.2023.e14428
 - 23) Chandramohan, D., and K. Marimuthu. “Drilling of natural fiber particle reinforced polymer composite material.” International Journal of Advanced Engineering Research and Studies, 1 (1):134–45. (2011).
 - 24) Anil K C, Kumaraswamy, Mahadeva Reddy, Bhograj Prakash, “Mechanical behavior and fractured surface analysis of bauxite residue and graphite reinforced aluminum hybrid composites” Fracture and Structural Integrity, 62, 168-179 (2022) <https://DOI: 10.3221/IGF-ESIS.62.12>.
 - 25) Akash, Anil.K.Chikkanna, Girisha.K.G, K.V.Sreenivas Rao “Effect of Fibre Orientation on Specific Gravity, Hardness, Flexural Strength and Tensile Properties of Jute/Hemp Hybrid Laminate Composite” Applied Mechanics and Materials Vol.

- 766-767, Trans Tech Publications, Switzerland, 75-78, (2015).
- 26) Anil Kumar, Kapil Dev, Ashish Dahiya, "Fabrication and Mechanical Characterization of Pomegranate Peel Powder mixed Epoxy Composite" EVERGREEN Joint Journal of Novel Carbon Resource Sciences & Green Asia Strategy, 10 (04), 2173-2179, (2023), <https://doi.org/10.5109/7160892>.
- 27) Anil Kumar, Jayant P. Supale, Kavita Goyal, "Fabrication and Material Characterization of Composite Fiberboard made by Walnut's Waste", EVERGREEN Joint Journal of Novel Carbon Resource Sciences & Green Asia Strategy, 10 (04), 2153-2160, (2023), <https://doi.org/10.5109/7160890>
- 28) Praveen Saraswat, Naveen Kumar Sain, Dheeraj Joshi, Sandeep Kumar Bhaskar, "Experimental Investigation of Float Glass in Rotary Ultrasonic Machining for Sustainable Manufacturing", EVERGREEN Joint Journal of Novel Carbon Resource Sciences & Green Asia Strategy, 10 (04), 2520-2527, (2023), <https://doi.org/10.5109/7162018>
- 29) Harishchandra, R.S. Kadadevaramath and K.C. Anil, "Effect of tool material on machinability of TiCp reinforced Al-1100 composite" IOP Conf. Series: Materials Science and Engineering 149 012026. (2016), DOI:10.1088/1757-899X/149/1/012026
- 30) Anil.K.C, M.G. Vikas, Shanmukha Teja.B, K.V. Sreenivas Rao, "Effect of cutting parameters on surface finish and machinability of graphite reinforced Al-8011matrix composite" Materials Science and Engineering, 191 (2017) 012025. DOI:10.1088/1757-899X/191/1/012025
- 31) Latha Shankar, B.;Nagaraj, P. M.;Anil, K. C " Optimization of Wear Behaviour of AA8011-Gr Composite using Taguchi Technique" Materials Today: Proceedings, 4, 10739-10745. (2017), DOI: 10.1016/j.matpr.2017.08.021
- 32) Harini Sosiati, Yankeisna Auda Shofie and Aris Widyo Nugroho, "Tensile Properties of Kenaf/Eglass Reinforced Hybrid Polypropylene (PP) Composites with Different Fiber Loading" EVERGREEN Joint Journal of Novel Carbon Resource Sciences & Green Asia Strategy, 05(02),1-5,(2018), <https://doi.org/10.5109/1936210>
- 33) Asad Aslam Shaikh, Atharva Anil Pradhan, Atharva Mahesh Kotasthane, Santosh Patil, Saravanan Karuppanan, "Comparative analysis of Basalt/EGlass/S2-Fibreglass-Carbon fiber reinforced epoxy laminates using finite element method, Materials Today: Proceedings, 63, 630- 638, (2022), <https://doi.org/10.1016/j.matpr.2022.04.385>.
- 34) Baldev Singh Rana, Gian Bhushan, Pankaj Chandna "The Impact of Nano Fly Ash Particulates on Tribological Performance of Jute /Cotton fiber Reinforced Hybrid Biocomposite" EVERGREEN Joint Journal of Novel Carbon Resource Sciences & Green Asia Strategy, 10, (03), 1349-1356, (2023), <https://doi.org/10.5109/7151682>
- 35) Anil Kumar, Sonu Singh, "Fabrication and Optimization of Wear Behaviour of Citrus Limetta Peel Particulate Composite using Hybrid Taguchi- GRA-PCA" , EVERGREEN Joint Journal of Novel Carbon Resource Sciences & Green Asia Strategy, 10,(03), 1323-1329, (2023), <https://doi.org/10.5109/7151679>